Compensation of shallow impurities in oxygen-doped metalorganic vapor phase epitaxy grown GaAs

J. W. Huang,[a] K. L. Bray, and T. F. Kuech[b]
Department of Chemical Engineering, University of Wisconsin, Madison, Wisconsin 53706

(Received 2 July 1996; accepted for publication 3 September 1996)

Intentional oxygen incorporation, using diethyl aluminum ethoxide $[(C_2H_5)_2AlOC_2H_5]$ during metalorganic vapor phase epitaxy GaAs was found to compensate C and Zn shallow acceptors as well as Si and Se shallow donors, due to the oxygen-related multiple deep levels within the GaAs band gap. Deep level transient spectroscopy (DLTS) was used to characterize the energy levels associated with these oxygen deep centers. The total measured trap concentration from DLTS can account for the observed compensation in *n*-type GaAs:O. The total trap concentration in *p*-type GaAs:O, however, was found to be lower than the observed compensation by a factor of ~100. These oxygen deep centers exhibit multiple electronic states which have been associated with the local number of Al nearest neighbors and the microscopic structure of the defect. The concentration and nature of these deep levels were not influenced by the chemical identity of the shallow dopants.
 [S0021-8979(96)01524-1]

I. INTRODUCTION

Metalorganic vapor phase epitaxy (MOVPE) is widely used to grow high purity $Al_xGe_{1-x}As$ and high quality $Al_xGa_{1-x}As$/GaAs interfaces, both of which are important in many optoelectronic and digital device structures. The growth of $Al_xGa_{1-x}As$, however, has always been difficult due to the reactive nature of both the Al-bearing alkyls and the $Al_xGa_{1-x}As$ growth surface. The initial studies of MOVPE $Al_xGa_{1-x}As$ have often reported materials that exhibited a low photoluminescence (PL) efficiency and a reduced free electron concentration, when co-doped with shallow donors.[1,2] Both observations have been attributed to the incorporation of oxygen that results in deep level centers. These defects or defect complexes are effective nonradiative recombination centers, reducing the PL efficiency, and can compensate the shallow donors. Recently, Chen *et al.*[3] reported the deep level transient spectroscopy (DLTS) spectrum of a Zn doped $Al_{0.2}Ga_{0.8}As$ layer, exhibiting five different hole traps which were attributed to unintentional oxygen incorporation. The tendency of the oxygen deep centers to be electrically and optically active in both *n*- and *p*-type $Al_xGa_{1-x}As$, however, is not presently understood.

Alkoxide contaminants in the metalorganic precursors [such as trimethyl aluminum (TMAl) and trimethyl gallium (TMGa)] and trace levels of H_2O and O_2 in the process gases are cited as sources of residual oxygen incorporation into $Al_xGa_{1-x}As$.[4] In the latter case, it has been postulated that the oxygen incorporation results from the *in situ* O_2-TMAl gas phase reaction forming volatile dimethyl aluminum methoxide $[(CH_3)_2AlOCH_3$ (DMALO)].[5] This alkoxide then acts as a gas phase oxygen source. In contrast, the intentional oxygen introduction, by the addition of H_2O or O_2 to the growth ambient during GaAs MOVPE growth, does not lead to oxygen incorporation.[2,6] The direct, independent introduction of DMALO[7,8] or diethyl aluminum ethoxide $[(C_2H_5)_2AlOC_2H_5)$(DEALO)],[9] however, has been demonstrated to result in controlled oxygen incorporation in GaAs. The trace amounts of Al, derived from Al in these oxygen precursors, on the growth surface or in the gas phase provide active sites for oxygen incorporation. Oxygen is subsequently incorporated into the growing crystal through the formation of a strong Al–O bond leading to Al–O based defects. These Al–O based defects in GaAs have been shown to give rise to multiple deep levels within the GaAs band gap,[7–10] and compensate shallow Si[7,9] and Te[8] donors. It would be of great interest to examine if similar compensation, in intentionally oxygen-doped GaAs, occurs in *p*-type materials. Such studies can provide a comparison with the behavior of oxygen in *p*-type $Al_{0.2}Ga_{0.8}As$ layers,[3] and should lead to a better understanding, in the electrical characteristics, of this oxygen-doped MOVPE GaAs material.

Numerous efforts have been made to minimize the unintentional oxygen incorporation in MOVPE $Al_xGa_{1-x}As$, such as the removal of oxygen-containing impurities from the precursors[11] and the carrier gas. A new approach has been recently reported to achieve a deep level free MOVPE $Al_{0.22}Ga_{0.78}As$ layer through the use of a low level of Se doping ($\sim 1 \times 10^{17}$ cm^{-3}).[12,3] The disappearance of oxygen-related deep level peaks in the DLTS spectra has been attributed to the passivation of the oxygen deep centers through the formation of a Se–O containing defect complex. The mechanism of this passivation is not understood nor has this effect of Se been widely confirmed. An equivalent study is presented here whereby the oxygen and Se concentration in the GaAs are independently controlled.

This article presents a comparative study of the compensation of shallow acceptors and shallow donors in DEALO-doped GaAs grown by MOVPE. Specifically, C and Zn were used for *p*-type doping, and Si and Se for *n*-type doping. The compensation, if it occurs, should be mainly attributed to the Al–O based defects.[10,8] Nevertheless, the possible interactions between oxygen and shallow dopants in the gas phase or near the growth front cannot be excluded, *a priori*. While

[a]Present address: Hewlett-Packard Company, Optoelectronics Division, San Jose, CA 95131.
[b]Electronic mail: kuech@engr.wisc.edu

other dopant-oxygen complexes, such as the Zn–O complex in GaP,[13] have been observed, we have studied a variety of shallow dopants in order to provide direct evidence of any possible oxygen-dopant interactions in our films.

II. EXPERIMENTAL PROCEDURES

All samples were grown in a conventional horizontal low pressure (78 Torr) MOVPE reactor,[9] using TMGa and arsine (AsH_3), on Si- or Zn-doped n^+ or p^+ (100) GaAs substrates with a 2° miscut in [010] direction toward (110) plane. Disilane (Si_2H_6), hydrogen selenide (H_2Se), dimethyl zinc (DMZn), and carbon tetrachloride (CCl_4) were employed for Si, Se, Zn, and C, doping, respectively, in the form of dilute (<25 ppm), high pressure gas mixtures with high purity hydrogen. DEALO was used for oxygen incorporation in a standard bubbler configuration.[9] The growth temperature was 600 °C and the V/III ratio was 40 for all samples. The growth rate was held constant at 0.05 μm/min, corresponding to a TMGa mole fraction of $\sim 1.8 \times 10^{-4}$ within the reactor.

Electrical and physical characterizations were carried out on multilayer samples that were grown using a growth sequence in which the shallow dopant or oxygen precursor mole fractions were varied in a stepwise fashion. A growth-property relationship can then be obtained from a single growth experiment by using secondary ion mass spectroscopy (SIMS) and electrochemical capacitance–voltage (*EC–V*) profiling analysis. The physical concentration depth profiles of oxygen and aluminum, as well as the shallow dopants, in these multilayer structures were obtained from SIMS. *EC–V* measurements rendered the net ionized impurity concentration ($N_d - N_a$ in *n*-type GaAs or $N_a - N_d$ in *p*-type GaAs) depth profiles. Additional samples possessing a single epitaxial layer were also grown for DLTS experiments. Au (for *n*-type GaAs) or Al (for *p*-type GaAs) Schottky contacts, 500 μm in diameter, were deposited using a standard lithography and lift-off process. Conventional DLTS scans were performed using double boxcar correlators.[10] The trap concentration, N_T, was estimated by the expression[14]

$$N_T = 2(N_d - N_a)\frac{\Delta C}{C} f(W), \tag{1}$$

where

$$f(W) = \frac{1}{\left(\frac{W-\lambda}{W}\right)^2 - \left(\frac{W_p-\lambda_p}{W}\right)^2}. \tag{2}$$

$N_d - N_a$ is determined by a *C–V* measurement on the Schottky diode. *C* is the diode capacitance under the quiescent reverse bias condition, and ΔC is the capacitance change in the transient due to complete trap filling during the pulse. $\Delta C/C$ must be less than 0.1 for Eq. (1) to hold. *W* and W_p in Eq. (2) are junction depletion widths under reverse bias and during the pulse, respectively. *W*-λ is the distance from *W* where the deep level, E_T, crosses the Fermi level, E_F. The term λ has been shown to be[14]

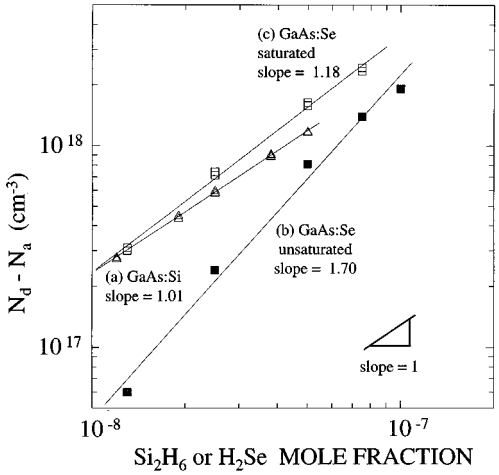

FIG. 1. The $N_d - N_a$ in GaAs via Si doping using Si_2H_6 and via Se doping using H_2Se are shown as a function of Si_2H_6 and H_2Se mole fractions in the gas phase. (a) A linear relationship was observed for Si doping (Δ). (b) A superlinear relationship (power law with an exponent of 1.7) was observed for an early run when the flow path was not saturated with Se (■). (c) A linear relationship was observed for a later run when the flow path was saturated with Se (□).

$$\lambda = \sqrt{\frac{2\epsilon\epsilon_0(E_F - E_T)}{q^2(N_d - N_a)}}, \tag{3}$$

where q is the elementary charge, ϵ is the static dielectric constant of GaAs, and ϵ_0 is the free space permittivity. The term $f(W)$ in Eq. (1) arises from the fact that not all volume of the depletion layer contributes to ΔC. Appreciable error in the determination of the trap concentration was found to occur by neglecting this edge region effect since $f(W)$ was sometimes much greater than 1. All trap concentration results presented here have been corrected for this effect. The trap energies are unaffected by this correction.

III. RESULTS

A. Initial experiments

The controlled incorporation of the shallow dopants was established prior to the oxygen co-doping experiments. The preferred *n*-type species in GaAs is Si due to its low diffusion coefficient and low volatility. The linear relationship between $N_d - N_a$ in the GaAs and the Si_2H_6 mole fraction was observed in the *EC–V* profiles, as shown in Fig. 1(a).[9] The use of H_2Se has been shown to exhibit a ''memory effect,'' which was attributed to H_2Se adsorption onto the internal walls of the growth system and its subsequent desorption after the nominal source shutoff.[15] The resulting free electron concentration was also found to have a superlinear (order ~1.5) relationship with respect to the H_2Se mole fraction in the gas phase.[16] The dependence of $N_d - N_a$ in GaAs on the H_2Se mole fraction in our reactor is shown in Fig. 1. An early calibration run [Fig. 1(b)] established a 1.7-order relationship, similar to the reported value of 1.5. $N_d - N_a$, however, was found to increase when using the same H_2Se mole fraction in later runs, and the net carrier concentration eventually leveled off at a particular value. A second calibration run, after the steady state doping effi-

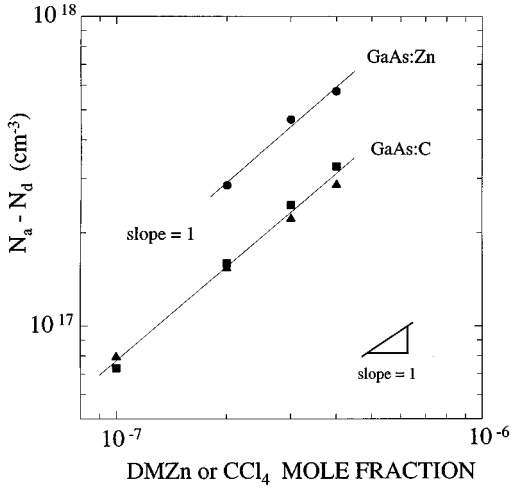

FIG. 2. The $N_a - N_d$ in GaAs via Zn doping using DMZn and via C doping using CCl_4 are shown as a function of DMZn and CCl_4 mole fractions in the gas phase. A linear relationship is noted for both cases.

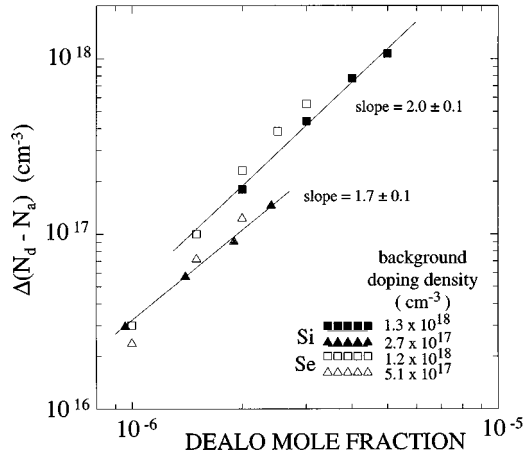

FIG. 3. The reduction of $N_d - N_a$ in GaAs as a function of DEALO mole fraction at different background donor concentrations of Si or Se. The least-squares fitting lines (see Ref. 18) are based on the data of the Si-doped samples. The effect of background donor concentration levels on the compensation is noted, independent of the type of shallow donors.

ciency was reached, as shown in Fig. 1(c), exhibited a close-to-linear relationship. These observations could be attributed to the saturation of adsorbed H_2Se in the delivery pipeline after a certain number of growth runs. In this article, all the reported results associated with Se doping were taken from samples grown after the saturation was reached to ensure reproducibility.

Zn doping using DMZn is also reported to exhibit a memory effect,[17] similar to the case of H_2Se. The measured $N_a - N_d$ as a function of DMZn mole fraction was, however, found to be linear, as shown in Fig. 2, indicating no such memory effect in our reactor. The preferred *p*-type dopant, however, is *C*, due to its low solid state diffusion coefficient, as well as the absence of any memory effect when using CCl_4.[17] A linear $N_a - N_d$ relationship on CCl_4 mole fraction relationship was noted, in Fig. 2, from a calibration sample grown in our reactor.

B. DEALO-doped n-type GaAs

Si donors in GaAs are compensated by oxygen-related deep level centers.[9] These results on Si and oxygen co-doped samples have been presented, in part, elsewhere.[9] Additional data and the presentation of these results are given here as a comparison to the new data on the Se, Zn, and C co-doping experiments. The SIMS Si concentration in one of the multilayer samples was found to be constant at 1.32×10^{18} cm^{-3}, and the Si doping efficiency from Si_2H_6 was not altered by the presence of DEALO. The compensation, $\Delta(N_d - N_a) = (N_d - N_a)_{\text{no oxygen}} - (N_d - N_a)_{\text{oxygen}}$, is shown in Fig. 3 as a function of the DEALO mole fraction. A power-law dependence, with the compensation being approximately[18]

$$\Delta(N_d - N_a) \propto [\text{DEALO}]^2, \tag{4}$$

is noted. The results from a similar sample, grown with a lower Si concentration at 2.73×10^{17} cm^{-3}, are also shown in Fig. 3. An approximate second-order power-law dependence is also observed from that sample. It is noted that the use of a greater amount of Si may appear to lead to a greater $\Delta(N_d - N_a)$ under the same DEALO concentration, as indicated by the two separate lines in Fig. 3. The limited data in Fig. 3, however, are not sufficient to verify the presence of this possible minor trend of compensation on Si concentration.

The Si_2H_6 mole fraction for each sample in Fig. 3 was kept constant throughout the growth resulting in a constant Si concentration. Additional samples were grown in which the concentration of DEALO remained constant while that of Si_2H_6 was varied during growth. Results from a typical sample grown under this type of growth condition are shown in Fig. 4(a), where DEALO was used for the growth of material only over the depth range of 1–2.9 μm. A clear compensation effect was noted over this region. The doping efficiency of Si remains the same regardless of the presence of DEALO. The incorporation of O and Al from DEALO is also not altered over the entire range of Si_2H_6 mole fractions [Fig. 4(b)]. The sharp turn-on and turn-off profiles of Al and O in Fig. 4(b) are also noted, indicating the absence of any memory effect when DEALO is applied as an oxygen precursor. The oxygen levels outside of these regions are limited by the SIMS resolution limits.

The defect structure responsible for the aforementioned compensation was investigated by using DLTS to determine the underlying deep level electronic characteristics. Two single-layer GaAs:Si:O samples were grown, and the sample specifications and their DLTS spectra are given in Figs. 5(a) and 5(b). Multiple deep levels are present in both samples, similar to the results we have previously reported using a p^+-n homojunction diode.[10] The deep level characteristics of sample (a), shown in Table I, were determined from Fig. 5(a) and a standard Arrhenius plot.[10,18] The total trap concentration, N_T, of sample 5(a) can account for the observed compensation within a factor of ~3. Comparison of the total N_T of sample 5(a) with its total SIMS oxygen concentration ($\sim 1.5 \times 10^{16}$ cm^{-3})[10] also indicates a close agreement. The approximate agreement, most probably within the combined

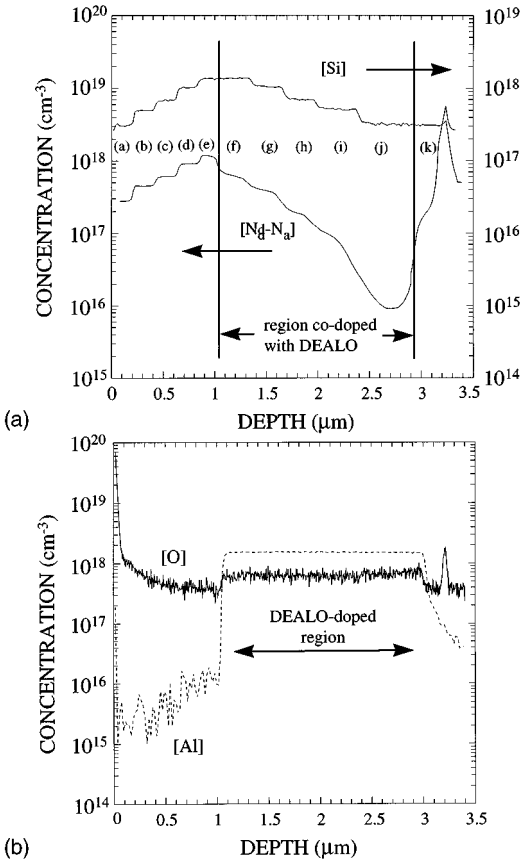

FIG. 4. (a) Profiles of SIMS Si and EC–V $N_d - N_a$ of a GaAs multilayer sample. DEALO mole fraction is kept constant at $3 \times 10^{-6}$from (f) to (j). Si_2H_6 mole fraction for each layer is: (a) 1.2×10^{-8}, (b) 1.9×10^{-8}, (c) 2.5×10^{-8}, (d) 3.8×10^{-8}, (e) 5×10^{-8}, (f) 5×10^{-8}, (g) 3.8×10^{-8}, (h) 2.5×10^{-8}, (i) 1.9×10^{-8}, (j) 1.2×10^{-8}, and (k) 1.2×10^{-8}. (b) Corresponding profiles of SIMS Al and O.

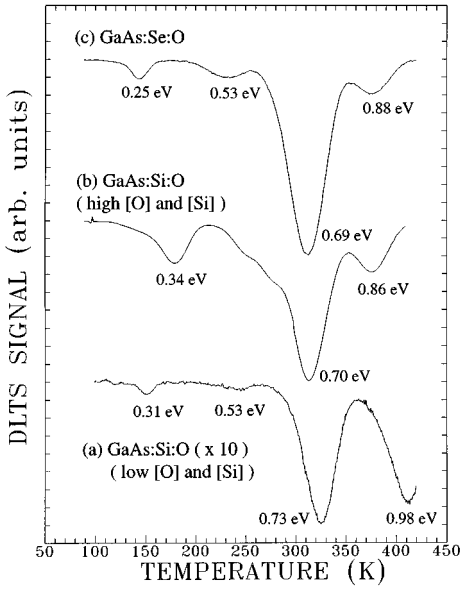

FIG. 5. DLTS spectra of DEALO and Si_2H_6 or H_2Se co-doped GaAs. DEALO mole fractions are: (a) 1.5×10^{-6}, (b) 5×10^{-6}, and (c) 2×10^{-6}. Si_2H_6 mole fractions are: (a) 5×10^{-9} and (b) 5×10^{-8}. H_2Se mole fraction for (c) is 2.5×10^{-8}. The terms $\Delta(N_d-N_a)$ for samples a, b, and c are 3×10^{16}, 8×10^{17}, and 4.3×10^{17} cm^{-3}, respectively. Similar multiple deep level structures are noted for all cases, and spectra peak heights are found to be approximately proportional to $\Delta(N_d-N_a)$. Measurement conditions are: reverse bias -1 V, pulse height 1 V, pulse width 1 ms for (a) and (c), and 0.1 ms for (b), pulse period 500 ms, and rate window 11.63 s^{-1}.

experimental uncertainty of our measurements, between compensation, the total N_T, as well as the SIMS oxygen concentration, supports the contention that oxygen-induced, acceptor-like deep levels are responsible for the compensation. Sample (b) has a more than one order of magnitude increase in compensation (8×10^{17} cm^{-3}) as compared to that of sample (a) (3×10^{16} cm^{-3}). This increase is reflected by the ~ten times increase in the DLTS peak heights. While the general shape of spectrum (b) stays unchanged, when compared to (a), a shift of the major deep level energy positions to lower emission energies is noted. The reasons for this shift are not presently clear.

A similar compensation effect, as in the case of Si, was observed [Fig. 6(a)] when Se was used as the shallow *n*-type dopant. The Se incorporation, at a concentration of 1.23×10^{18} cm^{-3}, was not affected by the variation of DEALO concentrations [Fig. 6(b)]. According to the EC–V results of Fig. 6(a), a ~second-order power-law dependence of the compensation on the DEALO mole fraction, as given by Eq. (4), is also noted in Fig. 3 for this Se-doped sample. The results from a second similar sample grown with a lower Se concentration at 5.14×10^{17} cm^{-3} are also shown in Fig. 3. An additional sample, grown under a constant DEALO mole fraction but varying the Se concentration, is given in Fig. 7. The results obtained for both Si and Se are very similar, indicating that DEALO and Si_2H_6 or H_2Se do not appreciably interact to form dopant-oxygen defect complexes during the MOVPE GaAs growth.

The DLTS analysis on a GaAs:Se:O Au-Schottky diode sample is shown in Fig. 5(c). The amount of compensation in this sample, $\Delta(N_d - N_a) \sim 4.3\times10^{17}$ cm^{-3}, is comparable to that of sample (b) in Fig. 5, and is approximately equal to the total N_T calculated from the DLTS peak heights (Table I). The Arrhenius plots of its four peaks also give rise to very similar energy levels to sample (b) in Fig. 5, as compared to those of sample (a). The measured defect structure is therefore very similar regardless of the use of Si or Se.

C. DEALO-doped *p*-type GaAs

The DEALO doping was found to lead to compensation in *p*-type GaAs, as indicated in Fig. 8 for a carbon and oxygen co-doped multilayer GaAs sample. The carbon concentration for this sample, obtained from SIMS measurements, is constant throughout at 2.9×10^{17} cm^{-3} with step changes in the oxygen concentrations. The carbon doping efficiency from CCl_4 is therefore not altered by the presence of DEALO. The measured electrical compensation from Fig. 8 is shown in Fig. 9 as a function of the DEALO mole fraction. A nonlinear power-law dependence of the electrical compensation on the DEALO mole fraction is again noted, as in the case of *n*-type GaAs. The results from a second similar sample grown with a higher carbon concentration at 9.73×10^{17} cm^{-3} are also shown in Fig. 9. These samples

TABLE I. Deep level characteristics of GaAs:Si:O [sample (a) of Fig. 5] and GaAs:Se:O [sample (c) of Fig. 5]. $N_d - N_a$ were determined by C–V measurement on Au Schottky diodes at room temperature. Trap cross section areas σ were obtained from intercepts of Arrhenius plots. The total N_T is noted to be very close to $\Delta(N_d - N_a)$. The high uncertainty in the cross section is a result of the limited data range.

Sample	$N_d - N_a$ ($\times 10^{16}$ cm^{-3})	$\Delta(N_d - N_a)$ ($\times 10^{16}$ cm^{-3})	ΔE_T (eV)	σ ($\times 10^{-14}$ cm)	N_T ($\times 10^{16}$ cm^{-3})	Total N_T ($\times 10^{16}$ cm^{-3})
5(a)	6.5	3	0.309±0.006	4.0±1.7	0.02	0.94
Si			0.531±0.013	6.3±3.7	0.02	
			0.728±0.012	9.8±3.8	0.42	
			0.981±0.038	31±33	0.48	
5(c)	17	43	0.251±0.007	0.18±0.11	0.91	42.1
Se			0.529±0.032	22±35	0.56	
			0.689±0.033	7.5±8.9	16.6	
			0.880±0.035	24±25	24.0	

possess a two slope behavior over the investigated range of DEALO gas phase mole fractions. The origin of this change in slope is not understood at present.

The underlying deep level structure responsible for this *p*-type compensation, as measured by DLTS, is shown in Figs. 10(a) and 10(b) for two single-layer GaAs:C:O samples. The DLTS spectra exhibit a multiple-level structure, similar to the reported spectrum of $Al_{0.2}Ga_{0.8}As$:Zn:O.[3] All the peak heights in the spectra of GaAs:C:O samples increase with the DEALO mole fraction at a constant carbon concentration. Four separate deep level peaks in these spectra are identified and analyzed. The deep level characteristics of sample (b) are tabulated in Table II. In contrast to the *n*-type case with the same DLTS measurement conditions, the total N_T for GaAs:C:O cannot account for all the observed compensation, and is smaller than $\Delta(N_a - N_d)$ by a factor of ~100.

The zinc acceptors are also compensated due to oxygen doping, as shown in Fig. 9, with very similar compensation results to the case of GaAs:C:O. This finding indicates that

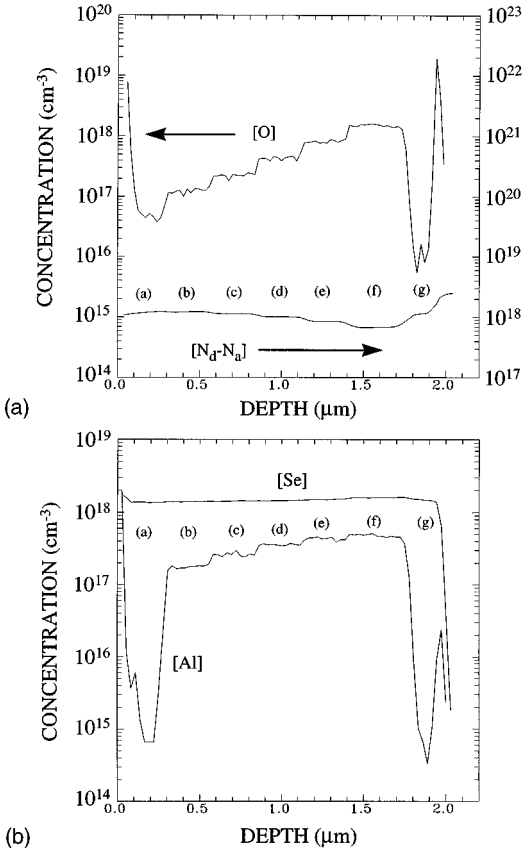

FIG. 6. (a) Profiles of SIMS O and EC–V $N_d - N_a$ of a GaAs multilayer sample. H_2Se mole fraction is kept constant at 3.8×10^{-8} throughout. DEALO mole fraction in each layer is (a) 0, (b) 1×10^{-6}, (c) 1.5×10^{-6}, (d) 2×10^{-6}, (e) 2.5×10^{-6}, (f) 3×10^{-6}, and (g) 0. (b) Corresponding profiles of SIMS Se and Al.

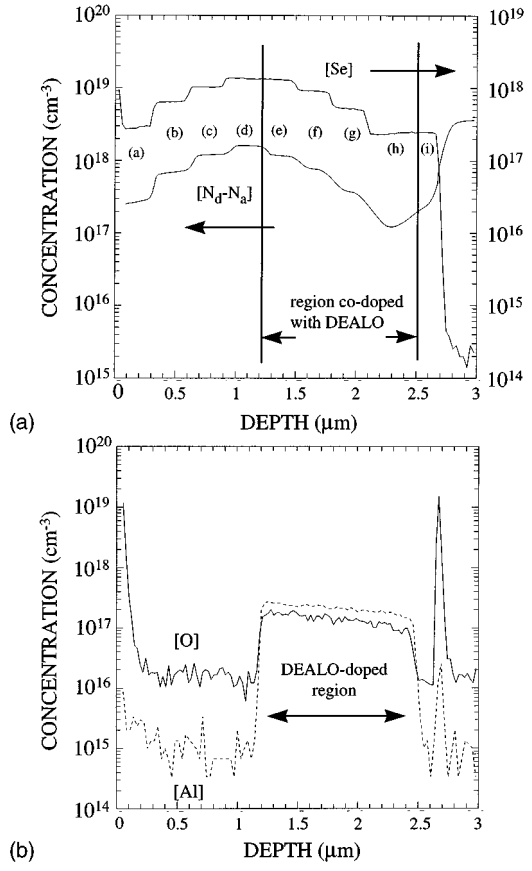

FIG. 7. (a) Profiles of SIMS Se and EC–V $N_d - N_a$ of a GaAs multilayer sample. DEALO mole fraction is kept constant at $2\times10^{-6}$from (e) to (h). H_2Se mole fraction for each layer is: (a) 1.3×10^{-8}, (b) 2.5×10^{-8}, (c) 3.8×10^{-8}, (d) 5×10^{-8}, (e) 5×10^{-8}, (f) 3.8×10^{-8}, (g) 2.5×10^{-8}, (h) 1.3×10^{-8}, and (i) 1.3×10^{-8}. (b) Corresponding profiles of SIMS Al and O.

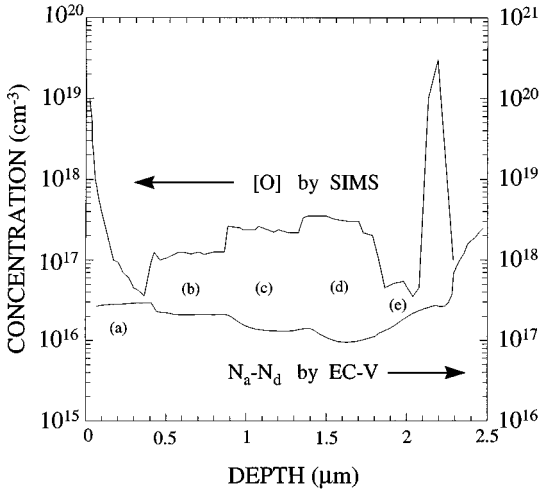

FIG. 8. The profiles of SIMS oxygen and EC–V $N_a - N_d$ of a GaAs multilayer sample indicate that the reduced $N_a - N_d$ is directly correlated with the enhanced oxygen incorporation at higher DEALO mole fractions. CCl_4 mole fraction is kept constant at 4×10^{-7} throughout. DEALO mole fraction in each layer is (a) 0; (b) 2×10^{-6}, (c) 3×10^{-6}, (d) 4×10^{-6}, and (e) 0.

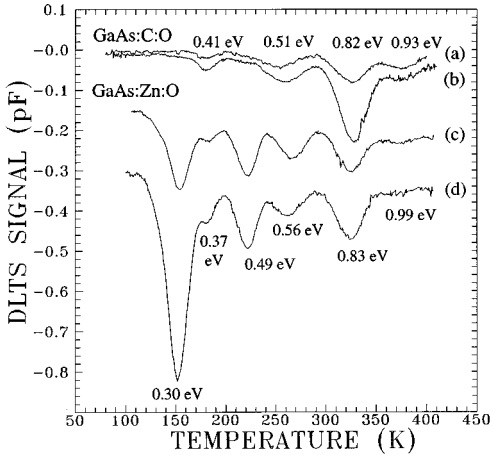

FIG. 10. DLTS spectral of DEALO and CCl_4 or DMZn co-doped GaAs. The spectra of (c) and (d) have been shifted by -0.15 and -0.3 pF, respectively. DEALO mole fractions are: (a) and (c): 3×10^{-6}, (b) and (d): 4×10^{-6}. CCl_4 and DMZn mole fractions are 4×10^{-7} and 2×10^{-7}, respectively. The terms $\Delta(N_a - N_d)$ for samples a, b, c, and d are 1.62×10^{17}, 1.98×10^{17}, 1.7×10^{17}, and 2.2×10^{17} cm^{-3} based on EC–V measurements. Similar multiple deep level structures are noted for all cases. Measurement conditions are: reverse bias -1V, pulse height 1 V, pulse width 1 ms, pulse period 500 ms, and rate window 4.65 s^{-1}.

the type of shallow acceptors does not affect the degree of compensation. The DLTS spectra of GaAs:Zn:O, illustrated in Figs. 10(c) and 10(d), exhibit similar multiple-level features as in GaAs:C:O. Two additional peaks are resolved in Figs. 10(c) and 10(d), along with all the deep level peaks of GaAs:C:O with comparable peak heights. The deep level characteristics of the sample in Fig. 10(d) are summarized in Table II. Again, the total N_T of GaAs:Zn:O in Table II cannot account for all the observed compensation, smaller by a factor of $\sim$60 to $\Delta(N_a - N_d)$, similar to the GaAs:C:O case. The general features of the deep level structure in p-type GaAs:O are therefore independent of the chemical character of the shallow acceptor.

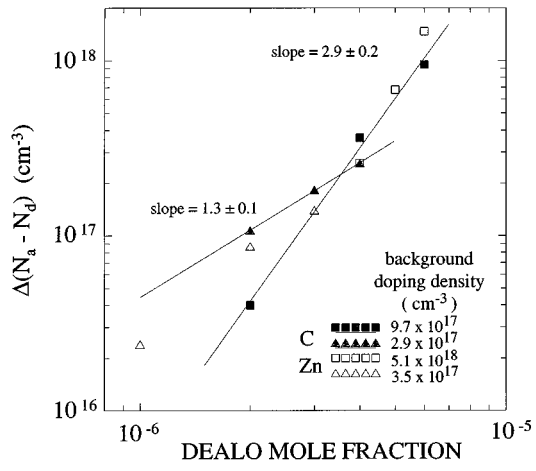

FIG. 9. The reduction of $N_a - N_d$ as a function of DEALO mole fraction at different background acceptor concentrations of C or Zn. The least-squares fitting lines (see Ref. 18) are based on the data of the C-doped samples. The effect of background acceptor concentrations on compensation is noted, independent of the type of shallow acceptors.

IV. DISCUSSION

In this study, the DEALO-doped GaAs epitaxial layers, co-doped with a wide variety of shallow dopants, exhibited a comparable amount of dopant compensation in both n- and p-type cases, as a similar concentration of DEALO was applied during the growth (Figs. 3 and 9). DLTS measurements on these materials have identified deep levels in both n- and p-type materials which are responsible for the observed compensation (Tables I and II). In the case of n-type GaAs, the concentration of deep levels determined from DLTS quantitatively agreed with the observed trap-induced compensation levels. The measured total trap concentrations in p-type GaAs:O was found to be lower than the observed compensation by a factor of $\sim$100. It is not unlikely that the presence of additional levels in p-type GaAs:O with very large emission time constants, which are beyond our DLTS measurement capability, could account for part of the discrepancy. On the other hand, the unaccounted compensation could also have resulted from the unsaturated hole trap centers in p-type GaAs:O under our DLTS pulsing conditions. An increase of the pulse duration from 1 ms (Fig. 10) to a longer period of time space, beyond the range of our instrumentation, could have better saturated the hole traps, leading to an increased DLTS signal and higher inferred trap concentration. More studies are needed to resolve this issue.

The chemical identity of shallow donors/acceptors does not appear to have a role in the amount of electrical compensation, as indicated in Figs. 3 and 9. Additionally, very similar DLTS spectra were found on samples (b) and (c) of Fig. 5, as well as samples (b) and (d) of Fig. 10, indicating that the type of shallow donors/acceptors does not affect the deep level characteristics. All the spectral features in Figs. 5 and 10 should therefore be dominated by the Al–O based centers due to DEALO doping. The possible formation of such spe-

TABLE II. Deep level characteristics of GaAs:C:O [sample (b) of Fig. 10] and GaAs:Zn:O [sample (d) of Fig. 10]. $N_a - N_d$ were determined by C–V measurement on Al Schottky diodes at room temperature. Trap cross section areas σ were obtained from intercepts of Arrhenius plots. The total N_T is noted to be lower than $\Delta(N_a - N_d)$ by a factor of ~100. The high uncertainty in the cross section is a result of the limited data range.

Sample	N_a-N_d ($\times 10^{16}$ cm^{-3})	$\Delta(N_a-N_d)$ ($\times 10^{16}$ cm^{-3})	ΔE_T (eV)	σ ($\times 10^{-14}$ cm^2)	N_T ($\times 10^{14}$ cm^{-3})	Total N_T ($\times 10^{14}$ cm^{-3})
10(b)	5	24	0.414±0.011	2.9±1.8	1.9	26
C			0.514±0.013	0.04±0.02	3.4	
			0.818±0.024	12±9	15	
			0.930±0.060	6.8±12	5.3	
10(d)	4.3	25	0.299±0.014	0.07±0.06	12	39
Zn			0.372±0.016	0.14±0.13	3.7	
			0.490±0.014	0.71±0.46	6.4	
			0.559±0.012	0.12±0.05	3.9	
			0.827±0.014	15±7	9.2	
			0.986±0.050	39±58	3.8	

cies as Si–O or Se–O can therefore be ruled out as contributing to the observed deep level structure in this low Al composition $Al_xGe_{1-x}As$, or more accurately Al-doped GaAs. Park and Skowronski[8] have reported the DLTS spectra of GaAs:Te:O using DMALO as the oxygen precursor. Their DLTS spectra, obtained from two samples with compensation levels of 5.2×10^{16} and 7×10^{16} cm^{-3}, are quite similar to the spectrum of sample (a) in Fig. 5 with a compensation of 3×10^{16} cm^{-3}. The Te–O bond strength (93.4 kcal/mol) is weaker than that of Si–O (191 kcal/mol) and Se–O (101 kcal/mol),[19] and thus no interactions between Te and O are expected or were found in that study.[8]

The SIMS results of Figs. 4, 6, and 7 also indicate that the shallow donors and oxygen precursors do not interact with each other in the gas phase or in the crystal, leading to the independent incorporation of Si (or Se) and O in GaAs. Such gas phase interactions are unlikely due to the low concentration of the reactants in the reactor ambient. It should be pointed out that the compensation effect as observed here in the Se and O co-doped GaAs is inconsistent with the report on the passivation effect of Se doping in $Al_xGa_{1-x}As$,[12] which has been attributed to the possible reduction of the electrically active Al–O species due to the formation of the electrically inactive Al–Se bond or a Al–O–Se related complex. The electrical deactivation of the oxygen-related defects, if it occurs, should give rise to a reduced compensation in the presence of Se in our DEALO-doped GaAs, as compared to GaAs:Si:O in Figs. 3 and 4. The compensation in our GaAs:Se:O samples, shown in Figs. 3, 6, and 7, is, however, quite similar to GaAs:Si:O. In the discussion presented in the previous study of the Se doping of low oxygen content $Al_xGa_{1-x}As$[3] has suggested the formation of Se–Al bonds, in preference to Al–O bonds, or Al–O–Se complexes based on bond strength arguments. Both mechanisms are suggested to lead to electrically inactive oxygen in the crystal as opposed to the removal of oxygen from the growth front. Given the much stronger Al–O (122 kcal/mol) bond over that of Al–Se (80 kcal/mol),[19] such bond strength arguments are probably too simplistic to adequately describe these effects. Additionally, the oxygen-related deep levels in GaAs and $Al_xGa_{1-x}As$ appear to be very similar in nature to our work as well as others.[2,7–10,20,21] If such a Se-doping effect leading to the improvement of the electrical and optical properties $Al_xGa_{1-x}As$ is substantiated, the microscopic mechanism of the impact of Se on these films is quite puzzling and deserves further investigation.

The striking similarity, in the compensation behavior and the multiple deep level structure, of oxygen deep centers in both *p*- and *n*-type GaAs suggests that these deep centers can have a variety of charge states, capturing both electrons and holes. The distribution of charge states over the defect population depends on the Fermi level position, which is in turn governed by the intentional shallow impurity doping and the oxygen concentration. While the specific microscopic nature of the oxygen-related deep centers is not presently understood, an analogy may be drawn from the electronic states associated with the lattice vacancy in silicon (V_{Si}).[22] An isolated V_{Si} gives rise to four dangling bonds, each containing one electron which may occupy a lower energy configuration by forming new covalent bonds with the other neighboring atoms. The total defect energy may be lowered through a tetragonal Jahn–Teller distortion to overcome the electron–electron repulsion. V_{Si} hence can assume a variety of charge states by gaining or losing electrons. The presence of five charge states of V_{Si}, ranging from a double donor to a double acceptor, have been experimentally observed.[22] In bulk-grown GaAs, the electrically active oxygen defect is assumed to be an off-centered, substitutional oxygen on an arsenic vacancy (V_{As}–O complex) consisting of a ''Ga-O molecule'' and a Ga–Ga bridging bond.[23] In DEALO-doped GaAs, the Ga_2O molecule could be replaced by an $Al_xGa_{2-x}O$ species since the Al–O bonding is the main driving force for oxygen incorporation, with Ga–Ga, Al–Ga, or Al–Al back bridging bonds. We have previously attributed the observed multiple deep level structure in DEALO-doped GaAs to the variation in the number of Al nearest-neighbors to oxygen.[10] This identification is supported by the growth and incorporation behavior of oxygen from DEALO into GaAs.[24] The dangling bonds on the two constituents of the back bridging bond could be quite reactive, forming states quite similar in origin to the V_{Si}. As in the case of the V_{Si}, the Fermi level position determines the charge distribution with these defect states.

V. CONCLUSION

The intentional oxygen incorporation, using DEALO, in MOVPE GaAs was found to compensate C and Zn shallow acceptors as well as Si and Se shallow donors, due to the oxygen-related multiple deep levels within the GaAs band gap. DLTS was used to characterize these oxygen deep centers. No changes in compensation or the DLTS characteristics were detected by varying the chemical identities of the shallow dopants, and the possible interactions between these shallow impurities and oxygen are not present. In particular, the recently inferred complex of Se and O in $Al_xGa_{1-x}As$, leading to the lack of observed effects typically attributed to oxygen in these Se-doped materials, was not observed in our study. The total measured trap concentration from DLTS can account for the observed compensation only in *n*-type GaAs:O. The total trap concentration in *p*-type GaAs:O was found to be lower than the observed compensation by a factor of $\sim$100. These oxygen deep centers appear to be able to possess at least two net charge states, positive (donors) or negative (acceptors) in nature, that are both energetically favorable. These multiple charge states could have contributed, in part, to the multiple deep level structure of GaAs:O.

ACKNOWLEDGMENTS

The authors would like to thank T. J. Anderson and S. A. Stockman for technical assistance. The financial support of the Army Research Office, the Naval Research Laboratory, and the National Science Foundation are also gratefully acknowledged.

[1] G. B. Stringfellow and G. Hom, Appl. Phys. Lett. **34**, 794 (1979).
[2] R. H. Wallis, M.-A. di Forte Poisson, M. Bonnet, G. Beuchet, and J.-P. Duchemin, Inst. Phys. Conf. Ser. **56**, 73 (1981).
[3] J. C. Chen, Z. C. Huang, B. Yang, H. K. Chen, T. Yu, and K.-J. Lee, J. Electron. Mater. **24**, 1677 (1995).
[4] T. F. Kuech, E. Veuhoff, T. S. Kuan, V. Deline, and R. Potemski, J. Cryst. Growth **77**, 257 (1986).
[5] H. Terao and H. Sunakawa, J. Cryst. Growth **68**, 157 (1984).
[6] D. W. Kisker, J. N. Miller, and G. B. Stringfellow, Appl. Phys. Lett. **40**, 615 (1982).
[7] M. S. Goorsky, T. F. Kuech, F. Cardone, P. M. Mooney, G. J. Scilla, and R. M. Potemski, Appl. Phys. Lett. **58**, 1979 (1991).
[8] Y. Park and M. Skowronski, J. Appl. Phys. **76**, 5813 (1994).
[9] J. W. Huang, D. F. Gaines, T. F. Kuech, R. M. Potemski, and F. Cardone, J. Electron. Mater. **23**, 659 (1994).
[10] J. W. Huang and T. F. Kuech, Appl. Phys. Lett. **65**, 604 (1994).
[11] J. S. Roberts, J. P. R. David, T. E. Sale, and P. L. Tihanyi, J. Cryst. Growth **143**, 135 (1994).
[12] Z. C. Huang, B. Yang, H. K. Chen, and J. C. Chen, Appl. Phys. Lett. **66**, 2745 (1995).
[13] D. J. Wolford, S. Modesti, and B. G. Streetman, Inst. Phys. Conf. Ser. **65**, 501 (1982).
[14] Y. Zohta and M. O. Watanabe, J. Appl. Phys. **53**, 1809 (1982).
[15] C. R. Lewis, M. J. Ludowise, and W. T. Dietze, J. Electron. Mater. **13**, 447 (1984).
[16] R. W. Glew, Inst. Phys. Conf. Ser. **63**, 581 (1982).
[17] B. T. Cunningham, M. A. Haase, M. J. McCollum, J. E. Baker, and G. E. Stillman, Appl. Phys. Lett. **54**, 1905 (1989).
[18] P. R. Bevington, *Data Reduction and Error Analysis for the Physical Sciences* (McGraw-Hill, New York, 1969).
[19] *Lange's Handbook of Chemistry*, 14th ed., edited by John A. Dean (McGraw-Hill, New York, 1992), pp. 4–23.
[20] J. Lagowski, D. G. Lin, T. Aoyama, and H. C. Gatos, Appl. Phys. Lett. **44**, 336 (1984).
[21] S. T. Neild, M. Skowronski, and J. Lagowski, Appl. Phys. Lett. **58**, 859 (1991).
[22] G. D. Watkins, in *Deep Centers in Semiconductors: A State-of-the-Art Approach*, edited by S. T. Pantelides (Gordon and Breach, Philadelphia, 1992), p. 177.
[23] J. Schneider, B. Dischler, H. Seelewind, P. M. Mooney, J. Lagowski, M. Matsui, D. R. Beard, and R. C. Newman, Appl. Phys. Lett. **54**, 1442 (1989).
[24] T. F. Kuech, S. Nayak, J.-W. Huang, and J. Li, J. Cryst. Growth **163**, 171 (1996).